AUTHOR(S): ZHANG, J., XU, C., ZHANG, D., ZHAO, J., ZHENG, S., SU, H., WEI, F., YUAN, B. and FERNANDEZ, C.

TITLE: Facile synthesis of a nickel sulfide (NiS) hierarchical flower for the electrochemical oxidation of H2O2 and the methanol oxidation reaction (MOR).

YEAR: 2017

Publisher citation: ZHANG, J., XU, C., ZHANG, D., ZHAO, J., ZHENG, S., SU, H., WEI, F., YUAN, B. and FERNANDEZ, C. 2017. Facile synthesis of a nickel sulfide (NiS) hierarchical flower for the electrochemical oxidation of H2O2 and the methanol oxidation reaction (MOR). Journal of the electrochemical society [online], 164(4), pages B92-B96. Available from: https://doi.org/10.1149/2.0221704jes

OpenAIR citation: ZHANG, J., XU, C., ZHANG, D., ZHAO, J., ZHENG, S., SU, H., WEI, F., YUAN, B. and FERNANDEZ, C. 2017. Facile synthesis of a nickel sulfide (NiS) hierarchical flower for the electrochemical oxidation of H2O2 and the methanol oxidation reaction (MOR). Journal of the electrochemical society, 164(4), pages B92-B96. Held on OpenAIR [online]. Available from: https://openair.rgu.ac.uk

Facile Synthesis of a Nickel Sulfide (NiS) Hierarchical Flower for the Electrochemical Oxidation of H_2O_2 and the Methanol Oxidation Reaction (MOR)

Jingchao Zhang,[a] Chunying Xu,[a] Daojun Zhang,[a] Jingli Zhao,[a] Shuxian Zheng,[a] Huimin Su,[a] Feifei Wei,[a] Baiqing Yuan,[a,z] and Carlos Fernandez[b,z]

[a]*Henan Province Key Laboratory of New Optoelectronic Functional Materials, College of Chemistry and Chemical Engineering, Anyang Normal University, Anyang 455000 Henan, People's Republic of China*
[b]*School of Pharmacy and Life Sciences, Robert Gordon University, Aberdeen AB10 7GJ, United Kingdom*

The synthesis of a novel hierarchical flower-like NiS via a solvothermal method for the electrochemcial oxidation of H_2O_2 on a carbon paste electrode with high catalytic activity for the (MOR) in an alkaline medium has been reported. Novel nickel sulfide (NiS) hierarchical flower-like structures were characterized by X-ray diffraction, scanning electron microscope, and transmission electron microscopy. A carbon paste electrode was modified with the as-prepared hierarchical flower-like NiS, resulting in a high electrocatalytic activity toward the oxidation of H_2O_2. The NiS-modified electrode was used for H_2O_2 sensing, which was achieved over a wide linear range from 0.5 μM to 1.37 mM ($I/\mu A = -0.19025 + 0.06094$ C/mM) with a low limit of detection (LOD) of 0.3 μM and a limit of quantitation (LOQ) of 0.8 μM. The hierarchical flower-like NiS also exhibited a high electrocatalytic activity for the methanol oxidation reaction (MOR) in an alkaline medium with a high tolerance toward the catalyst-poisoning species generated during the MOR. The MOR proceeded via the direct electrooxidation of methanol on the oxidized NiS surface layer because the oxidation peak potential of the MOR was more positive than that of the oxidation of NiS.
 [DOI: 10.1149/2.0221704jes]

Manuscript submitted October 11, 2016; revised manuscript received January 11, 2017. Published January 24, 2017.

In recent years, a variety of metal sulfides nanostructures have been widely investigated due to their potential applications in energy storage and conversion devices, light-emitting diodes, photocatalytic and electrocatalytic reactions, sensors, thermoelectric devices, and memory devices.[1–8] Nickel sulfide (NiS), has been extensively used for dye-sensitized solar cells,[9] supercapacitors,[10] lithium ion batteries,[11] electrocatalysts[12] and photocatalysts[13] due to its high electronic conductivity, low cost, and simple production. Although numerous NiS compounds have been prepared using various morphologies such as: nanoframes,[14] hollow spheres,[15] core-shell structure,[16] nanorods,[17] nanoflake arrays,[18] nanosheets,[19] urchin-like micro/nanostructures,[20] the synthesis of hierarchical flower-like NiS has been limited.[21–23] In this work, we report the facile synthesis of NiS hierarchical flower-like nanostructures using a solvothermal route. The electrocatalytic performances of these NiS nanostructures were also investigated.

Hydrogen peroxide (H_2O_2) has attracted a great attention due to its importance as a reactive oxygen species and its involvement in chemical, biological, food-processing, medical, diagnostic, and environmental related fields.[24,25] Due to its key role, the determination of H_2O_2 have arisen a great interest, hence many approaches have been developed, such as optical, titration-based, and electrochemical methods.[26–28] Among these methods, electrochemical analysis is particularly promising due to its many advantages such as low cost, easy to manipulate and fast analysis.[29] Although many nanostructures-based electrocatalysts such as prussian-blue-grafted carbon nanotube/poly (4-vinylpyridine) composites,[30] gold nanostars,[31] dumbbell-like PtPd−Fe_3O_4,[32] hierarchical hollow mesoporous CuO microspheres,[33] mesoporous Co_3O_4 nanobelts and nano-necklaces,[34] Co_3O_4 nanowires supported on 3D N-doped carbon foam[35] have been employed for this purpose, the preparation of the hierarchical nanostructure with high surface area is still a challenge for fabricating an efficient sensing platform for H_2O_2.

Pt-based materials are currently the most common electrocatalysts used as anodes in direct methanol fuel cells (DMFC) due to their high electrocatalytic activities.[36,37] However, Pt suffers from a high price and tendency to be poisoned by CO that occupies the active sites of the Pt via adsorption and block the transportation of methanol in its oxidation, limiting its utility in commercial applications. Therefore, the development of cost effective catalysts is highly desirable. Ni-based compounds are interesting alternatives to Pt due to their relative low costs and high electrocatalytic activity, which have attracted considerable recent attention[38,39] due to the Ni (II)/Ni (III) redox reactions.[40] To the best of our knowledge, this is the first time that the synthesis of a novel hierarchical flower-like NiS via a solvothermal method for the electrochemical detection of H_2O_2 on a carbon paste electrode with high catalytic activity for the MOR in an alkaline medium has been reported. The high catalytic activity for the MOR of the NiS nanostructures as an effective electrocatalysts in an alkaline medium opens a new potential application in DMFC.

Experimental

Chemicals and solutions.—Nickel (II) acetylacetonate (99.99%) and sulfur powder (99%) were purchased from Alfa Co. and Aladdin Co., USA. Tetrabutylammonium bromide, n-hexane, triton X-100, dimethylacetamide, ethanol, and diethylamine were acquired from Sinopharm Chemical Reagent Co., Ltd, China. H_2O_2 (30%) was purchased from Sigma-Aldrich. All other chemicals were of analytical reagent grade, and doubly distilled water was used for solution preparation.

Apparatus.—The phase of the hierarchical flower-like NiS structure was determined on a Rigaku D/max2550VB X-ray diffractometer (XRD). Scanning electron microscopy (SEM) images were obtained with a Hitachi SU8010 scanning electron microscope. Transmission electron microscopy (TEM) images and high-resolution TEM (HRTEM) images were obtained on an FEI Tecnai G2 F20 transmission electron microscope at an accelerating voltage of 200 kV. The specific surface areas of the samples were measured by nitrogen adsorption on a Gemini VII 2390 Analyzer at 77 K using the volumetric method. A CHI 842C electrochemical workstation (Austin, TX, USA) was used for all electrochemical experiments with a conventional three-electrode system, which included a NiS-modified carbon paste electrode (CPE) as the working electrode, a platinum coil as an auxiliary electrode, and an Ag/AgCl (saturated KCl) as the reference electrode.

[z]E-mail: baiqingyuan1981@126.com; c.fernandez@rgu.ac.uk

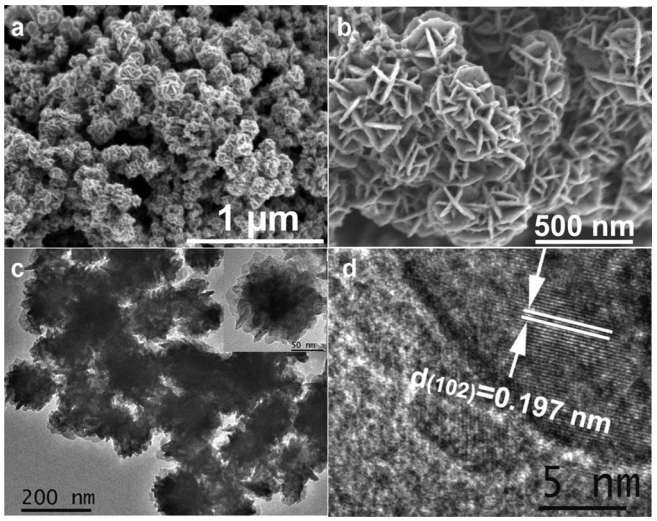

Figure 1. (a) Low-magnification and (b) high-magnification SEM image of NiS prepared at 200°C for 12 h. (c) TEM image of flower-like NiS nanostructures. (d) HRTEM image of a single NiS nanoflake.

Preparation of hierarchical flower-like NiS.—In a typical procedure, Nickel (II) acetylacetonate (0.1 mmol) and tetrabutylammonium bromide (0.15 mmol) was accurated weighted into a 20 mL teflon liner, and then dimethylacetamide (4.0 mL), ethanol (5.0 mL), H_2O (1.0 mL), Triton X-100 (1.0 mL), hexane (0.5 mL), and diethylamine (50 μL) was sucessively injected to form a micellar system under vigorous stirring. After stirring for 5 min, excessive sulfur power (4.8 mg) was then added to ensure the loss of sulfur during the reaction, and the mixture was stirred for 20 min. This mixture was transferred to a stainless steel autoclave, which was sealed, heated to 200°C, and maintained at this temperature for 12 h. The autoclave was cooled to room temperature, the upper layer yellow liquid has obvious stratification with the black solid deposited on the bottom. The liquid was pour away and the products were washed by ethanol and separated by centrifugation at 8000 rpm for 10 min, which ensured the full collection of the product. The black NiS powder can be ensured by being vacuum dried at 60°C for 1 h.

Fabrication of NiS modified CPE.—A carbon paste containing of 75:25 graphite powder/liquid paraffin, was packed firmly into one end of a glass tube (1.8 mm inner diameter) to fabiricate the bare CPE. Electronic connection to the CPE was made via a copper wire. To prepare NiS suspension, 2 mg NiS powder was ultrasonically dispersed in water for 10 minutes. For electrode modification, 5.0 μL of a NiS suspension (2 mg/mL) was drop-coated onto the bare CPE, which was then dried in an ambient atmosphere.

Results and Discussion

Characterization of the hierarchical flower-like NiS nanostructures.—Figs. 1a, 1b shows the typical SEM images of a NiS sample at different magnifications. Hierarchical flower-like structures with sizes ranging from 300 to 500 nm are clearly visible in the low-magnification SEM image. Meanwhile, the high-magnification image (Fig. 1b) reveals that these aggregates are composed of many uniformly distributed nanosheets with the thicknesses of ca. 18 nm. The structure of the flower-like NiS was further investigated by TEM (Fig. 1c) and HRTEM (Fig. 1d). According to these TEM images, the NiS product consisted of multiple nanosheets. The distance of the lattice finger is 0.197 nm, which corresponds to the d spacing of the (102) face of a hexagonal NiS phase (Fig. 1d).

Fig. 2a shows a typical XRD pattern of the NiS sample. The XRD pattern reveals the sample is highly crystalline. The four diffraction peaks at $2\theta = 30.2°$, 34.7°, 46.0°, and 53.5° can be indexed to the (100), (101), (102), and (110) planes, respectively, of the hexagonal NiS structure (JCPDS No.02-1280). No other impurity peaks were detected, indicating the high purity of the as-prepared NiS sample. An analysis of nitrogen adsorption isotherms (Fig. 2b) based on the Brunauer-Emmet-Teller theory indicated that the hierarchical flower-like NiS had a high surface area of 26.67 m^2/g and pore diameters of ~65 nm (inset to Fig. 2b).

Non-enzymatic H_2O_2 detection.—Next, we investigate the electroanalytical sensing of H_2O_2 using cyclic voltammetry. Fig. 3 shows typical cyclic voltammograms (CVs) recorded with a NiS-modified CPE in 0.1 M NaOH in the absence (dotted line) and presence (solid line) of 5 mM H_2O_2 over the potential range from −0.8 V to 0.8 V (vs. Ag/AgCl). A pair of redox peaks was observed at 0.5 V and 0.4 V, respectively. These peaks were attributed to the following redox reactions of NiS in an alkaline medium:[41]

$$NiS + OH^- = NiSOH + e^-$$

Accompanied by the addition of H_2O_2 to the solution, peaks for the oxidation and reduction of H_2O_2 appeared (solid line, Fig. 3), with an oxidation potential of 0.5 V and reduction potential of 0.6 V, respectively, suggesting that NiS was electrocatalytically active toward H_2O_2. The excellent electrocatalytic activity of the NiS-modified CPE

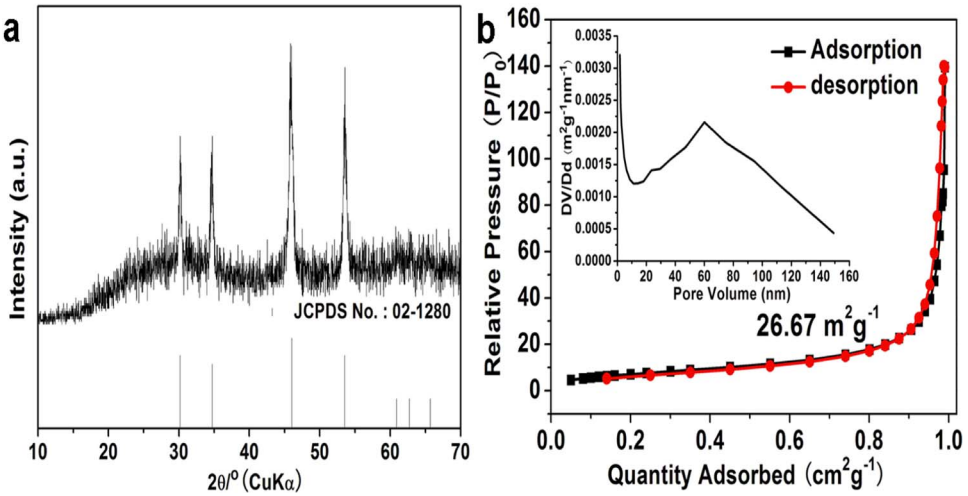

Figure 2. (a) XRD patterns of hierarchical flower-like NiS. Vertical lines (bottom) represent the typical pattern of the hexagonal NiS phase. (b) Nitrogen adsorption-desorption isotherm for the hierarchical flower-like NiS structures. *Inset*: BJH pore size distribution plot.

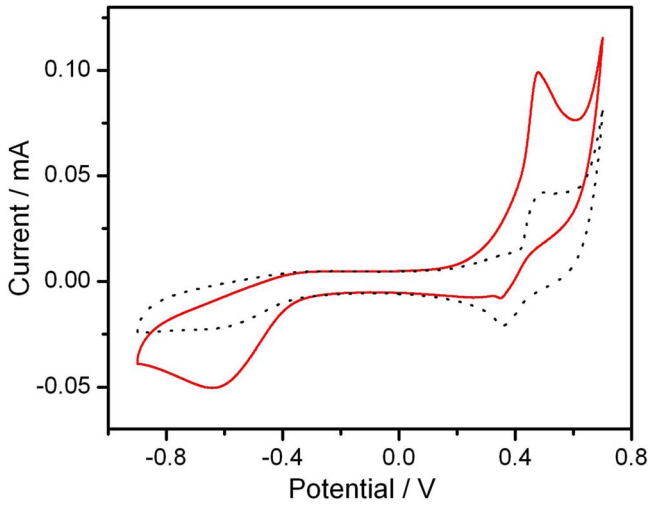

Figure 3. Typical CVs acquired at a NiS-modified CPE in 0.1 M NaOH in the absence (dotted line) and presence (solid line) of 5 mM H_2O_2 at a scan rate of 0.1 V/s. Arrow indicates the initial scan direction.

was also used for the amperometric detection of H_2O_2 (Fig. 4). H_2O_2 was successively injected into a stirred 0.1 M NaOH at an applied potential of 0.5 V. The measured current increased with H_2O_2 concentrations, and a linear response was observed from 0.5 μM to 1.37 mM ($I/\mu A = -0.19025 + 0.06094$ C/mM) with a low limit of detection (LOD) of 0.3 μM and a limit of quantitation (LOQ) of 0.8 μM. The H_2O_2 detection characteristics of the NiS-modified electrode and some other modified electrodes are compared in Table I. Overall, the NiS-modified electrode displayed a wider linear range and lower limit of detection for H_2O_2 than the other electrodes.

Reproducibility and repeatability tests of the NiS-modified electrodes revealed a relative standard deviation of 5.2% for ten successive measurements with the same electrode and 6.8% for measurements

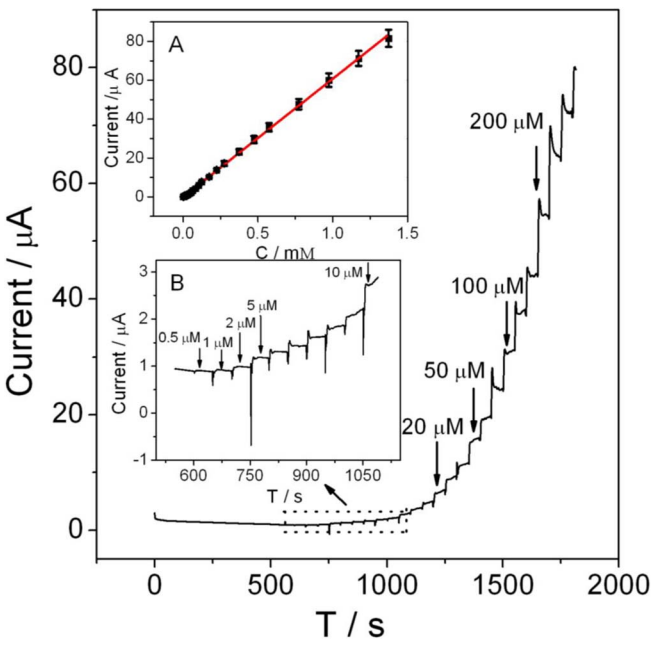

Figure 4. Amperometric response of the NiS-modified CPE to the successive addition of H_2O_2 in stirred 0.1 M NaOH at an applied potential of 0.5 V. *Insets*: magnified amperometric response to low H_2O_2 concentrations (A) and calibration curve for the steady-state current upon the addition of different H_2O_2 concentrations (B).

Table I. Comparative characteristics of the NiS-modified electrode and some other materials modified electrodes for the detection of H_2O_2 at an anodic potential.

Electrode material	Detection potential	Linear range/mM	LOD/μM	Ref.
$Pt_{0.5}Au_{0.5}$@C	0.3 V (Ag/AgCl)	0.007–6.5	2.4	42
Co_3O_4 nanoparticles	0.39 V(Ag/AgCl)	0.0004–2.2	0.105	43
MnOOH	0.45 V(Ag/AgCl)	0.02–9.67	3.2	44
Co_3O_4	0.5 V(Ag/AgCl)	0.005–0.35	0.7	45
PtIr nanoparticles	0.25 V(SCE)	0.1 –100	5	46
oxo-ruthenium(III)	0.56 V (SCE)	0.01–0.25		47
MnO_2/Au	0.7 V (SCE)	0.005–10	1	48
PtNi	0.7 V (RHE)	0.01–0.18	1	49
NiS	0.5 V (Ag/AgCl)	0.0005–1.37	0.3	This work

with five different electrodes, illustrating the acceptable reproducibilities and repeatabilities of the electrodes. The long-term stability of the NiS-modified electrode was also investigated under continuous operation. After 800 s of continuous operation, 88% of the initial current response was maintained. After being stored in air for two weeks, the electrode had an 8% decrease in current response, indicating its relatively high long-term stability.

The presented method was applied for the detection of H_2O_2 in disinfectant sample (2.7–3.3%). The disinfectant sample was diluted by water with a ratio of 1:30, after which 6.0 μL of the diluted sample solution was injected into the stirring 0.1 M NaOH solution (8 mL) and detected by amperometric method. The value of H_2O_2 concentration was found to be 2.9%, which was in accord with the value that obtained by permanganimetric method (3.1%).

Methanol electrooxidation.—The scan-rate dependence of the CVs of the NiS-modified CPE was also investigated, as shown in Fig. 5. Well-defined redox peaks were clearly observed at the different scan rate from 0.01 to 0.5 V/s and the currents increased proportionally with scan rate (I_{ox} (μA) = 35.35 + 355.67 υ; I_{red} (μA) = −1.97 – 115.72 υ), indicating that the processes were surface controlled according to the following Eqs. 1.

$$NiS + OH^- = NiSOH + e^- \quad [1]$$

The NiS-modified CPE was also used for the electrocatalytic oxidation of methanol. Fig. 6 shows CVs of the NiS-modified CPE in

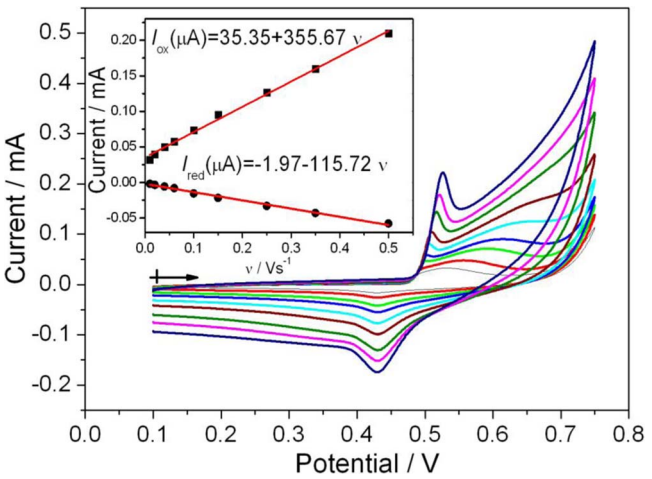

Figure 5. CVs of a NiS-modified CPE in 1.0 M KOH at different scan rates from 0.01 to 0.5 V/s. Arrow indicates the initial scan direction.

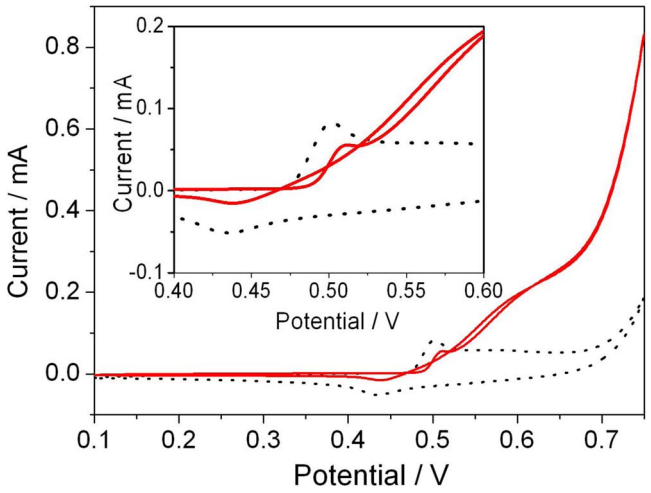

Figure 6. CVs of a NiS-modified CPE in 1.0 M KOH in the absence (dotted line) and presence (solid line) of 0.6 M methanol at a scan rate of 50 mV/s. Arrow indicates the initial scan direction.

1.0 M KOH in the absence (dotted line) and presence (solid line) of 0.6 M methanol at a scan rate of 50 mV/s. As shown in Fig. 6, no enhanced oxidation current appeared over the potential arrange before the oxidation peak potential of Ni (II)/Ni (III) (0.5 V) according to the following Eqs. 1. An obvious oxidation current was observed for MOR at the NiS-modified electrode when the potential was positive than 0.52 V, suggesting that direct electro-oxidation of methanol occurs after the oxidation of Ni (II) in which Ni (III) is used as an active surface for methanol oxidation. Similar oxidation currents were also observed during the reverse scan, these currents were ascribed to the further oxidation of methanol or other MOR intermediates. The forward and reverse oxidation currents nearly overlapped, suggesting that the NiS-modified electrode exhibited a high electrocatalytic activity for the MOR and a high tolerance for poisoning species generated by the MOR.

The CVs shown in Fig. 7, which were recorded at a scan rate of 50 mV/s, reveals the influence of the methanol concentration on the electrocatalytic activity of the NiS-modified. The anodic currents increase with the methanol concentration, suggesting that the oxidation

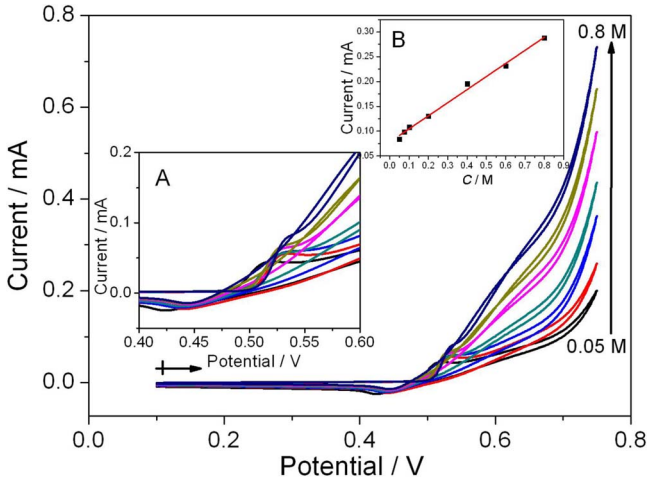

Figure 7. CVs of a NiS-modified CPE in 1.0 M KOH in the presence of different concentrations of methanol (0.05, 0.075, 0.10, 0.20, 0.40, 0.60, and 0.80 M) at a scan rate of 50 mV/s. Arrow indicates the initial scan direction. *Inset (A)*: The magnified CVs response at the potential range of 0.4–0.6 V. *Inset*: calibration plot of the oxidation peak current vs. methanol concentration. The current values are measured at 0.64 V.

of methanol exhibited a typical electrocatalytic response. Clearly, the anodic peak current in the forward sweep was proportional to the concentration of methanol. Another oxidation current was also observed in the reverse scan. This current also increased with the methanol concentration, suggesting that the methanol and other MOR intermediates that were partially oxidized in the forward scan were further oxidized during the reverse scan. In addition, the oxidation peak potential of the MOR (~0.52 V) was more positive than that of the oxidation of NiS (~0.5 V), indicating that the oxidation of methanol occurred through the direct electrooxidation on the Ni (III) surface via the following processes:[50,51]

$$Ni^{3+}\text{-methanol} = Ni^{3+}\text{-intermediate} + e^- \quad [2]$$

$$Ni^{3+}\text{-intermediate} = Ni^{3+}\text{-products} + e^- \quad [3]$$

Conclusions

Hierarchical flower-like NiS nanostructures were fabricated by a simple solvothermal method. The as-prepared NiS flower-like nanostructures were used for enzyme-free H_2O_2 sensing and methanol electrooxidation in an alkaline medium. The H_2O_2 sensor was highly reproducible and had an excellent electrocatalytic activity and a wide linear range from 0.5 μM to 1.37 mM. The hierarchical flower-like NiS also exhibited a high electrocatalytic activity for the methanol oxidation reaction (MOR) in an alkaline medium with a high tolerance toward the catalyst-poisoning species generated during the MOR. The MOR proceeded via the direct electrooxidation of methanol on the oxidized NiS surface layer.

Acknowledgments

Financial support is gratefully acknowledged from the National Science Foundation of China (No. 21405005, 21501006), the Joint Fund for Fostering Talents of National Natural Science Foundation of China and Henan Province (No. U1404208), the Program for Science and Technology Innovation Talents at the University of Henan Province (17HASTIT001), the Scientific Research Foundation for Returned Overseas Chinese Scholars, State Education Ministry.

References

1. M. R. Gao, Y. F. Xu, J. Jiang, and S. H. Yu, "Nanostructured metal chalcogenides: synthesis, modification, and applications in energy conversion and storage devices," *Chem. Soc. Rev.* **42**, 2986 (2013).
2. X. Huang, Z. Y. Zeng, and H. Zhang, "Metal dichalcogenidenanosheets: preparation, properties and applications," *Chem. Soc. Rev.* **42**, 1934 (2013).
3. C. L. Tan and H. Zhang, "Two-dimensional transition metal dichalcogenidenanosheet-based composites," *Chem. Soc. Rev.* **44**, 2713 (2015).
4. X. Y. Yu, L. Yu, and X. W. (David) Lou, "Metal sulfide hollow nanostructures for electrochemical energy storage," *Adv. Energy Mater.* **6**, 1501333 (2016).
5. H. J. Li, Y. Zhou, W. G. Tu, J. H. Ye, and Z. G. Zou, "State-of-the-art progress in diverse heterostructured photocatalysts toward promoting photocatalytic performance," *Adv. Funct. Mater.* **25**, 998 (2015).
6. Q. P. Lu, Y. F. Yu, Q. L. Ma, B. Chen, and H. Zhang, "2D Transition-metal-dichalcogenide-nanosheet-based composites for photocatalytic and electrocatalytic hydrogen evolution reactions," *Adv. Mater.* **28**, 1917 (2016).
7. D. Voiry, J. Yang, and M. Chhowalla, "Recent strategies for improving the catalytic activity of 2DTMD nanosheetstoward the hydrogen evolution reaction," *Adv. Mater.*, **28**, (2016)DOI: 10.1002/adma.201505597.
8. Y. W. Liu, C. Xiao, M. J. Lyu, Y. Lin, W. Z. Cai, P. C. Huang, W. Tong, Y. M. Zou, and Y. Xie, "Ultrathin Co_3S_4 nanosheets that synergistically engineer spin statesand exposed polyhedra that promote water oxidation under neutral conditions," *Angew. Chem. Int. Ed.* **54**, 11231 (2015).
9. X. W. Wang, B. H. Batter, Y. Xie, K. Pan, Y. P. Liao, C. M. Lv, M. X. Li, S. Y. Sui, and H. G. Fu, "Highly crystalline, small sized, monodisperse a-NiSnanocrystal ink as an efficient counter electrode for dye-sensitized solar cells," *J. Mater. Chem. A* **3**, 15905 (2015).
10. F. Cai, R. Sun, Y. R. Kang, H. Y. Chen, M. H. Chen, and Q. W. Li, "One-step strategy to a three-dimensional NiS reduced graphene oxide hybrid nanostructure for high performance supercapacitors," *RSC Adv.* **5**, 23073 (2015).

11. H. Geng, S. F. Kong, and Y. Wang, "NiS nanorod-assembled nanoflowers grown on graphene: morphology evolution and Li-ion storage applications," *J. Mater. Chem. A* **2**, 15152 (2014).
12. Y. B. Li, H. F. Wang, H. M. Zhang, P. R. Liu, Y. Wang, W. Q. Fang, H. G. Yang, Y. Lie, and H. J. Zhao, "A {0001} faceted single crystal NiS nanosheet electrocatalyst for dye-sensitised solar cells: sulfur-vacancy induced electrocatalytic activity," *Chem. Commun.* **50**, 5569 (2014).
13. Z. H. Chen, P. Sun, B. Fan, Z. G. Zhang, and X. M. Fang, "In situ template-free ion-exchange process to prepare visible-light-active g–C_3N_4/NiS hybrid photocatalysts with enhanced hydrogen evolution Activity," *J. Phys. Chem. C* **118**, 7801 (2014).
14. X. Y. Yu, L. Yu, H. B. Wu, and X. W. (David) Lou, "Formation of nickel sulfide nanoframes from metal-organic frameworks with enhanced pseudocapacitive and electrocatalytic properties," *Angew. Chem. Int. Ed.* **54**, 5331 (2015).
15. C. Z. Wei, C. Cheng, Y. Y. Cheng, Y. Wang, Y. Z. Xu, W. M. Du, and H. Pang, "Comparison of NiS_2 and α-NiShollow spheres for supercapacitors, non-enzymatic glucose sensors and water treatment," *Dalton Trans*. **44**, 17278 (2015).
16. S. S. Huang, K. D. M. Harris, E. Lopez-Capel, D. A. C. Manning, and D. Rickard, "Amorphous nickel sulfide" is hydrated nanocrystalline NiS with a core-shell structure," *Inorg. Chem.* **48**, 11486 (2009).
17. Q. Pan, J. Xie, T. J. Zhu, G. S. Cao, X. B. Zhao, and S. C. Zhang, "Reduced graphene oxide-induced recrystallization of NiS nanorodsto nanosheets and the improved Na-storage properties," *Inorg. Chem.* **53**, 3511 (2014).
18. X. Y. Yan, X. L. Tong, L. Ma, Y. M. Tian, Y. S. Cai, C. W. Gong, M. G. Zhang, and L. P. Liang, "Synthesis of porous NiS nanoflake arrays by ion exchange reaction from NiO and their high performance supercapacitor properties," *Mater. Lett.* **124**, 133 (2014).
19. N. D. Hoa, D. Van Thien, N. Van Duy, and N. Van Hieu, "Facile synthesis of single-crystal nanoporous α-NiSnanosheetsfrom $Ni(OH)_2$ counterpart," *Mater. Lett.* **161**, 282 (2015).
20. L. W. Mi, Y. F. Chen, W. T. Wei, W. H. Chen, H. W. Hou, and Z. Zheng, "Large-scale urchin-like micro/nano-structured NiS: controlled synthesis, cation exchange and lithium-ion battery applications," *RSC Adv*. **3**, 17431 (2013).
21. C. J. Tang, C. H. Zang, J. F. Su, D. M. Zhang, G. H. Li, Y. S. Zhang, and K. Yu, "Structure and magnetic properties of flower-like α-NiS nanostructures," *Appl. Surf. Sci.* **257**, 3388 (2011).
22. H. B. Li, L. L. Chai, X. Q. Wang, X. Y. Wu, G. C. Xi, Y. K. Liu, and Y. T. Qian, "Hydrothermal growth and morphology modification of α-NiS: three-dimensional flowerlike architectures," *Cryst. Growth Des.* **7**, 1918 (2007).
23. J. Q. Yang, X. C. Duan, Q. Qin, and W. J. Zheng, "Solvothermal synthesis of hierarchical flower-like β-NiS with excellent electrochemical performance for supercapacitors," *J. Mater. Chem. A* **1**, 7880 (2013).
24. M. Labib, E. H. Sargent, and S. O. Kelley, "Electrochemical methods for the analysis of clinically relevant biomolecules," *Chem. Rev.* **116**, 9001 (2016).
25. S. Abdellaoui, K. L. Knoche, K. Lim, and S. D. Minteer, "TEMPO as a promising electrocatalyst for the electrochemical oxidation of hydrogen peroxide in bioelectronic applications," *Journal of The Electrochemical Society*, **163**, H3001 (2016).
26. C. J. Lv, W. H. Di, Z. H. Liu, K. Z. Zheng, and W. P. Qin, "Luminescent $CePO_4$:Tb colloids for H_2O_2 and glucose sensing," *Analyst* **139**, 4547 (2014).
27. H. L. Tan, C. J. Ma, Q. Li, L. Wang, F. G. Xu, S. H. Chen, and Y. H. Song, "Functionalized lanthanide coordination polymernanoparticles for selective sensing of hydrogen peroxide in biological fluids," *Analyst* **139**, 5516 (2014).
28. W. Chen, S. Cai, Q. Q. Ren, W. Wen, and Y. D. Zhao, "Recent advances in electrochemical sensing for hydrogen peroxide: a review," *Analyst* **137**, 49 (2012).
29. M. M. Liu, R. Liu, and W. Chen, "Graphene wrapped Cu_2O nanocubes: non-enzymatic electrochemical sensors for the detection of glucose and hydrogen peroxide with enhanced stability," *Biosensors and Bioelectronics* **45**, 206 (2013).
30. J. Li, J. D. Qiu, J. J. Xu, H. Y. Chen, and X. H. Xia, "The synergistic effect of prussian-blue-grafted carbon nanotube/poly (4-vinylpyridine) composites for amperometric sensing," *Adv. Funct. Mater.* **17**, 1574 (2007).
31. Y. X. Li, J. Ma, and Z. F. Ma, "Synthesis of gold nanostars with tunable morphology and their electrochemical application for hydrogen peroxide sensing," *Electrochim. Acta* **108**, 435 (2013).
32. X. L. Sun, S. J. Guo, Y. Liu, and S. H. Sun, "Dumbbell-like PtPd−Fe_3O_4 nanoparticles for enhanced electrochemical detection of H_2O_2," *Nano Lett.* **12**, 4859 (2012).
33. S. Ghosh and M. K. Naskar, "A rapid one-pot synthesis of hierarchical hollow mesoporous CuO microspheres and their catalytic efficiency for the decomposition of H_2O_2," *RSC Adv.* **3**, 13728 (2013).
34. Q. Wang, Y. P. Xia, and C. L. Jiang, "Mesoporous nanobelts and nano-necklaces of Co_3O_4 converted from β-$Co(OH)_2$ nanobelts via a thermal decomposition route for the electrocatalytic oxidation of H_2O_2," *CrystEngComm* **16**, 9721 (2014).
35. M. M. Liu, S. J. He, and W. Chen, "Co_3O_4 nanowires supported on 3D N-doped carbon foam as an electrochemical sensing platform for efficient H_2O_2 detection," *Nanoscale*, **6**, 11769 (2014).
36. X. H. Sun, X. Zhu, N. Zhang, J. Guo, S. J. Guo, and X. Q. Huang, "Controlling and selfassembling of monodisperse platinum nanocubes as efficient methanol oxidation electrocatalysts," *Chem. Commun.* **51**, 3529 (2015).
37. Y. P. Zuo, K. Cai, L. Wu, T. T. Li, Z. C. Lv, J. W. Liu, K. Shao, and H. Y. Han, "Spiny-porous platinum nanotubes with enhanced electrocatalytic activity for methanol oxidation," *J. Mater. Chem. A* **3**, 1388 (2015).
38. L. Qian, W. Chen, R. F. Huang, and D. Xiao, "Direct growth of $NiCo_2S_x$ nanostructures on stainless steel with enhanced electrocatalytic activity for methanol oxidation," *RSC Adv*. **5**, 4092 (2015).
39. A. K. Das, R. K. Layek, N. H. Kim, D. Jung, and J. H. Lee, "Reduced graphene oxide (RGO)-supported $NiCo_2O_4$ nanoparticles: an electrocatalyst for methanol oxidation," *Nanoscale* **6**, 10657 (2014).
40. H. Huo, Y. Zhao, and C. Xu, "3D Ni_3S_2 nanosheet arrays supported on Ni foam for high-performance supercapacitor and nonenzymatic glucose detection," *J. Mater. Chem. A*, **2**, 15111 (2014).
41. P. K. Kannan and C. S. Rout, "High performance non-enzymatic glucose sensor based on one step electrodeposited nickel sulfide," *Chem. Eur. J.* **21**, 9355 (2015).
42. O. G. Sahin, "Microwave-assisted synthesis of PtAu@C based bimetallic nanocatalysts for non-enzymatic H_2O_2 sensor," *Electrochim. Acta* **180**, 873 (2015).
43. M. Wang, X. Jiang, J. Liu, H. Guo, and C. Liu, "Highly sensitive H_2O_2 sensor based on Co_3O_4 hollow sphere preparedvia a template-free method," *Electrochim. Acta* **182**, 613 (2015).
44. W. Xu, J. Liu, M. Wang, L. Chen, X. Wang, and C. Hu, "Direct growth of MnOOH nanorod arrays on a carbon cloth for high performance non-enzymatic hydrogen peroxide sensing," *Anal. Chim. Acta* **913**, 128 (2016).
45. C. Su, W. Lan, C. Chu, X. Liu, W. Kao, and C. Chen, "Photochemical green synthesis of nanostructured cobalt oxides as hydrogen peroxide redox for bifunctional sensing application," *Electrochim. Acta* **190**, 588 (2016).
46. S. Chang, M. Yeh, J. Rick, W. Su, D. Liu, J. Lee, C. Liu, and B. Hwang, "Bimetallic catalyst of PtIr nanoparticles with high electrocatalyticability for hydrogen peroxide oxidation," *Sens. Actuators B* **190**, 55 (2014).
47. M. F. S. Teixeira, F. H. Cincotto, and P. A. Raymundo-Pereira, "Electrochemical investigation of the dimeric oxo-bridged ruthenium complex inaqueous solution and its incorporation within a cation-exchange polymeric filmon the electrode surface for electrocatalytic activity of hydrogen peroxideoxidation," *Electrochim. Acta* **56**, 6804 (2011).
48. Y. Yang and S. Hua, "Electrodeposited MnO_2/Au composite film with improved electrocatalyticactivity for oxidation of glucose and hydrogen peroxide," *Electrochim. Acta* **55**, 3471 (2010).
49. C. Xu, J. Wang, and J. Zhou, "Nanoporous PtNi alloy as an electrochemical sensor for ethanol and H_2O_2," *Sens. Actuators B* **182**, 408 (2013).
50. R. H. Tammam, A. M. Fekry, and M. M. Saleh, "Electrocatalytic oxidation of methanol on ordered binary catalyst of manganese and nickel oxide nanoparticles," *Int. J. Hydrogen Energy* **40**, 275 (2015).
51. X. Cui, W. Guo, M. Zhou, Y. Yang, Y. Li, P. Xiao, Y. Zhang, and X. Zhang, "Promoting effect of Co in Ni_mCo_n (m + n = 4) bimetallic electrocatalysts for methanol oxidation reaction," *ACS Appl. Mater. Interfaces* **7**, 493 (2015).